An Assessment of Some Factors Influencing Multispectral Land-Cover Classification

Peng Gong and *Philip J. Howarth*
Earth-Observations Laboratory, Institute for Space and Terrestrial Science, Department of Geography, University of Waterloo, Waterloo, Ontario N2L 3G1, Canada

ABSTRACT: Experiments to evaluate the accuracies of different stages of land-cover classification are described. Four feature groups, two training strategies, three classifiers, and three accuracy assessment methods have been analyzed. The features used are three original SPOT HRV multispectral images, two principal component images and one edge-density image generated from the original multispectral Band 1 image. Single-pixel training and block training are evaluated. Classifiers used are the minimum Euclidian distance, the minimum Mahalanobis distance, and the maximum likelihood. Pure-pixel sampling, stratified random sampling, and stratified systematic unaligned sampling are used to generate Kappa coefficients for accuracy assessment. Results show that single-pixel training makes the largest contribution to improving classification accuracies. The second largest improvement results from use of the maximum-likelihood classifier rather than the minimum-Euclidian-distance classifier. The third largest contribution is from the inclusion of the edge-density image. Different sampling strategies used for accuracy assessment result in significantly different accuracy values measured by the Kappa coefficient.

INTRODUCTION

WITH THE ADVENT of higher spatial resolution remote sensing data, there is increasing interest in determining the most appropriate classification procedures for analyzing multispectral data. Not only are conventional procedures being considered, but also new algorithms based on contextual and texture measures are being proposed. To determine to what extent new classification algorithms are required, we need to have an in-depth understanding of the capabilities of conventional computer-assisted classification procedures. A review of the literature, however, indicates the lack of comprehensive evaluations on which this assessment can be made. In this paper, the aim is to evaluate some of the major procedures used at different stages of the classification process and to determine the most significant factors influencing the accuracies of conventional multispectral classification for land-cover mapping.

Image classification involves two phases. First is the design of the classification scheme. A general survey of the remote sensing literature shows that the most popular land-classification scheme is the one developed by Anderson *et al.* (1976). It is presented in detail in the *Manual of Remote Sensing* (Jensen, 1983) and in many remote sensing textbooks (e.g., Lillesand and Kiefer, 1987; Campbell, 1987). Other classification schemes are frequently based upon it. The land-use and land-cover classification system was proposed as a standard for manual interpretation by the United States Geological Survey. The rationale of the system is that human interpreters are capable of deriving both land-cover and land-use information by a series of inductions and deductions from the spatial composition of spectral signatures of various surface targets on an image. This can be done at different levels of detail, depending upon the scale of the data source being used and the level of detail required.

It is important to recognize, however, that the conventional computer-assisted classifiers (such as the maximum-likelihood classifier and the minimum-distance classifier) do not recognize spatial patterns in the same way that the human interpreter does. The classifiers perform class assignments based only on the spectral signatures of specific pixels. They do not take into account the locations of those pixels, nor the spectral characteristics of surrounding pixels. Bearing these in mind, to make better use of conventional computer-assisted classification methods, one must select a classification scheme in which classes are defined by spectral characteristics.

Previous studies have shown that a decrease in classification accuracy is likely to occur as the spatial resolution of the data are improved but other sensor characteristics are kept unchanged (Clark and Bryant, 1977; Townshend and Justice, 1981; Williams *et al.*, 1983; Toll, 1984; Toll, 1985; Latty *et al.*, 1985; Shimoda and Sakata, 1988; Howarth *et al.*, 1988; Martin *et al.*, 1988). In part, this can be attributed to the classification schemes used, because the integration of different land covers and land uses into one class will cause an increase of within-class variation. It is recognized that computer-assisted classification of remote sensing imagery is more appropriate for identifying and mapping land covers than it is for mapping land uses. For this reason, the emphasis of the work presented in this paper is on land-cover classification. In other words, the classification scheme used in this study consists of only spectral classes which are directly related to various land-cover types rather than land-use types. For land-use classification, another step has to be made to convert the land-cover types into more meaningful land-use types.

The second phase of image classification is the implementation of the classification scheme. In a typical computer-assisted classification, there are five major steps to be followed. These are

- Data preprocessing, including radiometric and geometric correction, feature selection, data reduction, and noise elimination.
- Training, involving either supervised or unsupervised training. Supervised training is the most commonly-used approach.
- Pixel labeling, which refers to the use of a classification algorithm to assign each image pixel to a class, according to the training statistics.
- Postprocessing for improving the visual appearance of the image. This includes filtering the classified results and performing geometric transformations depending on the application for the data.
- Accuracy assessment of the classified image compared with ground information. As discussed by Richards (1986) and Campbell (1987), there are many different ways to assess classification results.

In this study, a series of experiments has been undertaken to assess the effects of performance at each of the above five steps (except postprocessing) on classification accuracies. For each step, several approaches among the more popular ones were selected for evaluation. The experiments involved four different combinations of images, two procedures for supervised training, and the application of three kinds of conventional classi-

PHOTOGRAMMETRIC ENGINEERING AND REMOTE SENSING,
Vol. 56, No. 5, May 1990, pp. 597–603

0099-1112/90/5605–597$02.25/0

FIG. 1. A SPOT multispectral Band 1 image of part of the Markham study area. The area shown in the image is approximately 6 km by 8 km.

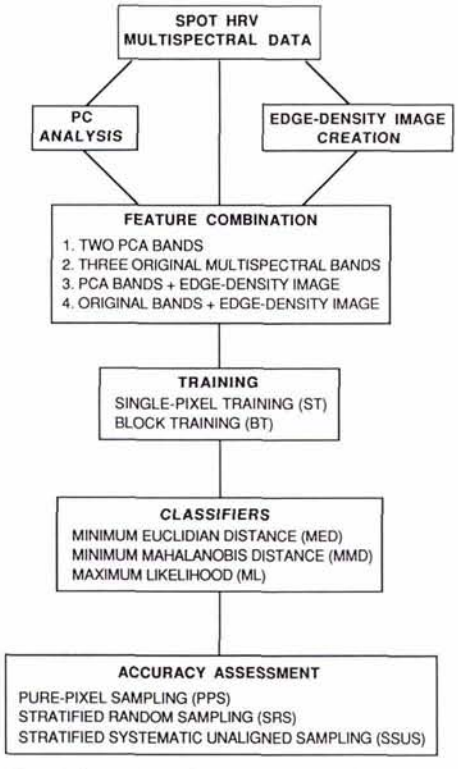

FIG. 2. An outline of the procedures followed in this study.

fiers. The results were then evaluated by means of three different accuracy assessment methods.

STUDY AREA AND DATA SOURCES

The area selected for study was the Town of Markham (43° 52′ N; 79° 15′ W), which is situated on the rural-urban fringe of northeastern Toronto. Land cover and land use in this area are typical of the rural-urban fringe of many cities in North America with agricultural and natural land being converted to primarily residential, industrial, and commercial uses. Over a number of years, several remote sensing studies of rural-to-urban land conversion have been carried out in this region (Martin, 1975; Martin, 1986; Johnson and Howarth, 1987; Howarth *et al.*, 1988; Martin *et al.*, 1988, Martin, 1989; Gong and Howarth, 1989; Gong and Howarth, 1990).

Data selected for this study consisted of SPOT High Resolution Visible (HRV) imagery recorded on 4 June, 1987. A 512- by 512-pixel subscene (approximately 10 km by 10 km) of multispectral (XS) data was chosen for the analysis. Figure 1 shows part of the study area (6 km by 8 km) with the built-up area at the lower portion of the figure. In addition, 1:8,000-scale panchromatic aerial photographs (taken less than two months before the imagery was recorded) were available to assist in land-cover identification.

METHODOLOGY

Analysis was carried out using software developed on a VAX 11/785 computer in FORTRAN 77. Image display was on a Dipix ARIES III image analysis system.

The type and sequence of procedures used in the analysis are outlined in Figure 2. As can be seen, at each of the major stages in the analysis different procedures were implemented and their results were compared. Details are presented below.

Land-Cover Classification Scheme

As discussed in the introduction, the classification scheme selected for the analysis was designed to display all the major land covers encountered in this area (Table 1). Four of them are primarily located in urban areas (the residential roof, the industrial and commercial roof, cleared land, and the lawn and tree complex), three are unique to rural areas (crop cover, new crop and pasture, and bare field), while the remaining five may be encountered in either environment (pavement surface, cultivated grass, deciduous trees, coniferous trees, and water).

Feature Combinations

In addition to the original three bands of the SPOT XS imagery, two types of derived images were incorporated into the analysis. First, a principal component analysis was undertaken. This was done because a correlation analysis of the three SPOT XS bands showed that the correlation between the two visible bands (Band 1 and Band 2) is over 0.98. The first two component images, which contain 99.6 percent of the total variance, were used in the analysis.

The second derived image was an "edge-density" image which was generated from the XS Band 1 image. This was done by first filtering the Band 1 image with a Laplacian operator to create an edge image. A threshold was then applied to this filtered image to obtain a binary edge image. By systematically moving a window over the binary edge image and determining the number of edge points, it was possible to generate the edge-density image which provides structural information in the classification. Further details are given in Gong and Howarth (1990).

Using the three sets of images, four feature combinations (Figure 2) were selected for the analysis. The rationale for these selections is that the three XS images form the basic data set, the two PCA images provide a reduced data set which could speed up analysis without loss of accuracy, and the combination of the edge-density image with the XS image and with the PCA image provides the incorporation of spatial structural information into the multispectral classification.

Training

Traditional supervised training involves the selection of contiguous pixels or blocks of pixel from representative locations across the image as training samples. This is referred to as block training (BT) and is one of the procedures evaluated in this paper (Figure 2). However, according to Campbell (1981) and Labovitz and Masuoka (1984), positive spatial autocorrelation exists among pixels which are contiguous or close together. The block training method violates the independent sampling requirement and therefore makes the training signatures for each class less representative. In order to avoid this problem, a sampling strategy using groups of single pixels was also included in this study. The training samples for each class were selected as individual pixels, but each pixel had to be at least several pixels away (usually more than ten pixels) from any other selected pixel. For both block training and single-pixel training (ST), the sample size for each class was approximately 60. This satisfies the requirement for a representative sample, as recommended by Swain and Davis (1978). The selection of training pixels was aided by reference to the 1:8,000-scale panchromatic aerial photographs of the study area.

The two kinds of training approach were applied to the four different feature combinations to provide eight sets of training statistics. Transformed divergence (TD) values were calculated according to the method described in Swain and Davis (1978). Each TD value indicates the separability between two training class signatures. The highest TD value is 2000 which indicates no spectral confusion between training classes. Usually a TD value higher than 1900 is desirable if confusion is to be avoided. For comparison of sets of training statistics, average TD values were calculated for each set.

Table 1. Land-Cover Types Used in the Classification

Residential Roof
Road Surface
Industrial and Commercial Roof
Cleared Land
Lawn and Tree Complex
Cultivated Grass
Deciduous Trees
Coniferous Trees
Crop Cover
New Crops and Pasture
Bare Field
Water Surface

Classification

The eight sets of training statistics were used with each of the three classifiers. Two of them are minimum-distance classifiers, with Euclidian distance and Mahalanobis distance as the measures, respectively. The other one is the standard maximum-likelihood classifier. Further details on these classifiers are to be found in Richards (1986).

Accuracy Assessment

Three sampling strategies were selected to test the accuracies of the classifications. In each case, the classified result from the image was compared with the same area on the ground by means of the 1:8,000-scale aerial photographs.

The first assessment was carried out using "pure-pixel" sampling (PPS). As with the single-pixel training, approximately 30 pixels for each class were selected as randomly as possible from throughout the image. Each test pixel used in the accuracy assessment had to have a unique ground cover that could be readily identified by the analyst using the 1:8,000-scale aerial photographs.

The second assessment involved using a stratified random sampling (SRS) strategy based on the thematic classes obtained from one of the classification results (Richards, 1986). Again, 30 test pixels for each class were obtained. Compared with the pure-pixel sampling, however, the analyst no longer had confidence that the correct class was identified for every test pixel. This was because in some cases the sampling method resulted in a mixed pixel being selected. In such cases, it is difficult to assign a single correct land cover to the pixel.

The third group of samples was selected using the stratified systematic unaligned sampling (SSUS) strategy (Jensen, 1983). In this procedure, a random sample is picked from every 16 by 16 stratum on the image. Consequently, in this case a total of 1024 samples was obtained. While identifying these samples, the analyst again encountered the problem of assigning the correct land cover to a mixed pixel.

After the test pixels were identified, the results were input to the computer. In this way, the classification results could be readily compared with the test results to generate statistics such as confusion matrices and accuracy measures. For this study, only the Kappa coefficient (Cohen, 1960) and its variance (Fleiss *et al.*, 1969) were used in the comparison. This coefficient has been recommended by Rosenfield and Fitzpatrick-Lins (1986) and Fung and LeDrew (1988) as a suitable accuracy measure in thematic classification for representing the whole confusion matrix. It takes all the elements in the confusion matrix into consideration rather than just the diagonal elements, as occurs with the calculation of overall classification accuracy.

RESULTS AND DISCUSSION

Training

Figure 3 shows the TD values obtained from applying two different kinds of training strategies to four groups of feature combination. In Figure 3, it can be seen, as expected, that in all cases the single-pixel training strategy produced higher TD values than the block training approach, when the same combination of features was being compared. It is also apparent that the two PCA images gave lower TD values than the original HRV image, whether or not the edge-density image was combined with the spectral bands. In both cases, the edge-density image improved the results of the class separability. This indicates that the inclusion of spatial information from the edge-density image is capable of increasing the class separability. The three XS bands combined with the edge-density image produced the highest TD values for both single-pixel training and block training.

Classification and Accuracy Assessment

In Table 2, the classification results evaluated using Kappa coefficients and their corresponding variances are summarized. Figures 4, 5, and 6 graphically present the Kappa coefficients for accuracy assessment results obtained using the minimum-Euclidian-distance (MED), minimum-Mahalanobis-distance (MMD), and maximum-likelihood (ML) classifiers, respectively. For each classifier, the effects of using the three different sampling strategies (PPS, SRS, SSUS), applied to the results of single-pixel training and block training, are displayed.

From Figure 4, it can be seen that, for all three accuracy-evaluation methods, single-pixel training resulted in higher classification accuracies than block training. Comparing the accuracy results for the two PCA bands with the original three XS bands, in all cases a small improvement of accuracy using the three XS bands is observed, except for block training and stratified systematic unaligned sampling. Both pure-pixel sampling and stratified systematic unaligned sampling show significant accuracy improvements when the edge-density image is included as one of the features in the classification, but this is not so apparent with stratified random sampling.

In both Figure 5, where the MMD classifier has been used, and Figure 6 based on the ML classifier, the results for single-pixel training again show higher accuracies than block training in all the combinations presented. Contrary to the results from the MED classifier, however, several cases occur where the two PCA bands show better results than the three XS bands, but there are exceptions. Use of the edge-density image improves results for pure-pixel sampling and stratified random unaligned sampling, but poorer results are observed with stratified random sampling based on block training.

From the evaluation, it is important to determine what contributes most to improved classification accuracy from among the feature combinations, the training procedures, and the classification algorithms. To determine this, the significance test proposed by Cohen (1960) for comparing two classification results was adopted. With this method, the difference between two Kappa coefficients resulting from two classifications is first obtained. The square-root of the sum of the variances between

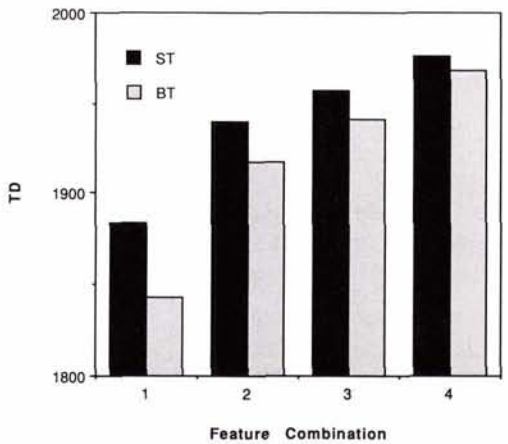

FIG. 3. Average transformed divergence (TD) values for the different feature combinations used in this study. In all cases single-pixel training produces higher TD values than block training. The feature combinations 1, 2, 3, and 4 and the abbreviations in the diagram are identified in Figure 2 and explained in the text.

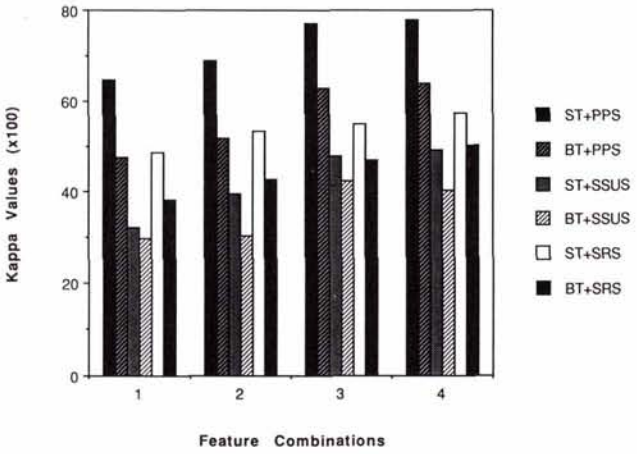

FIG. 4. The minimum-Euclidian-distance classification results obtained with the use of two training approaches applied to the four feature combinations and evaluated by the three accuracy-testing methods. Note that the highest accuracies are attained using single-pixel training applied to feature combinations including the edge-density image. The feature combinations 1, 2, 3, and 4 and the abbreviations in the diagram are identified in Figure 2 and explained in the text.

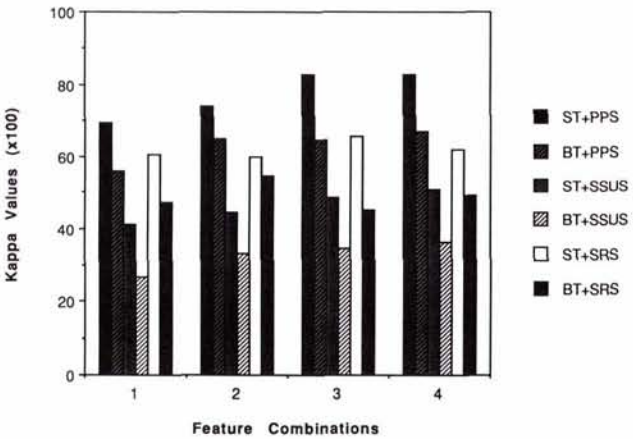

FIG. 5. The minimum-Mahalanobis-distance classification results obtained with the use of two training approaches applied to the four feature combinations and evaluated by the three accuracy-testing methods. Contrary to the results of the minimum-Euclidian-distance classifier, shown in Figure 4, there are several cases where the two PCA bands show better results than the XS bands. The feature combinations 1, 2, 3, and 4 and the abbreviations in the diagram are identified in Figure 2 and explained in the text.

TABLE 2. LAND-COVER CLASSIFICATION RESULTS MEASURED BY KAPPA COEFFICIENTS (KC) AND THEIR VARIANCE (VAR)

Training Mode	Classifier	Feature	PPS		SRS		SSUS	
			KC	VAR	KC	VAR	KC	VAR
BT	MED	1	0.475	0.00075	0.382	0.00082	0.299	0.00027
		2	0.518	0.00075	0.427	0.00082	0.304	0.00027
		3	0.629	0.00069	0.470	0.00083	0.424	0.00029
		4	0.638	0.00069	0.502	0.00081	0.405	0.00028
BT	MMD	1	0.561	0.00073	0.473	0.00078	0.267	0.00023
		2	0.649	0.00067	0.547	0.00078	0.334	0.00028
		3	0.645	0.00067	0.452	0.00079	0.345	0.00026
		4	0.669	0.00065	0.491	0.00078	0.362	0.00027
BT	ML	1	0.604	0.00071	0.562	0.00079	0.335	0.00028
		2	0.663	0.00066	0.619	0.00075	0.399	0.00029
		3	0.683	0.00064	0.551	0.00079	0.403	0.00028
		4	0.689	0.00063	0.550	0.00079	0.400	0.00029
ST	MED	1	0.646	0.00068	0.486	0.00079	0.321	0.00029
		2	0.689	0.00063	0.534	0.00078	0.396	0.00030
		3	0.770	0.00052	0.550	0.00080	0.477	0.00030
		4	0.778	0.00050	0.572	0.00078	0.491	0.00030
ST	MMD	1	0.693	0.00063	0.607	0.00077	0.414	0.00031
		2	0.738	0.00057	0.601	0.00077	0.445	0.00030
		3	0.830	0.00041	0.656	0.00072	0.485	0.00030
		4	0.830	0.00041	0.622	0.00075	0.508	0.00030
ST	ML	1	0.744	0.00056	0.625	0.00074	0.392	0.00031
		2	0.747	0.00056	0.632	0.00074	0.471	0.00031
		3	0.845	0.00038	0.669	0.00070	0.499	0.00030
		4	0.842	0.00039	0.644	0.00073	0.526	0.00030

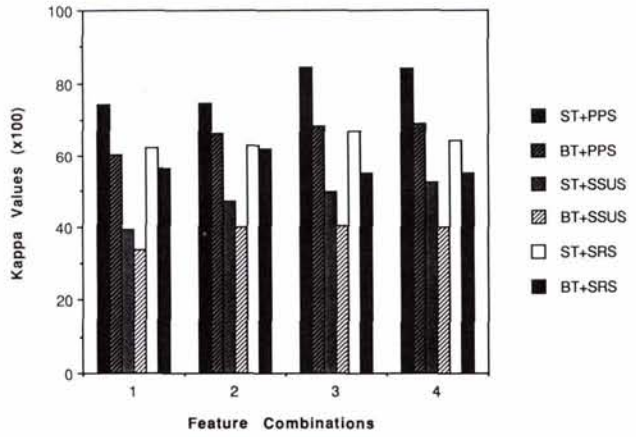

FIG. 6. The maximum-likelihood classification results obtained with the use of two training approaches applied to the four feature combinations and evaluated by the three accuracy-testing methods. The pattern of results is very similar to that shown in Figure 5. The feature combinations 1, 2, 3, and 4 and the abbreviations in the diagram are identified in Figure 2 and explained in the text.

the two classifications is then calculated. A Z-value can be determined by dividing the difference by the square-root of the sum of the variances. A Z-value above 1.96 indicates that the two classification results are significantly different at the 95 percent confidence level. In this study, the following strategies for each step in Figure 2 have been compared:

- Single-pixel training (ST) and block training (BT).
- The three-band XS image (F2) and the two-band PCA image (F1).
- The two-band PCA image plus the edge-density image (F3) and the three-band XS image (F2).
- The three-band XS image plus the edge-density image (F4) and the two-band PCA image plus the edge-density image (F3).
- Averages for F3 and F4 and averages for F1 and F2 to compare images with and without the edge-density image.
- The minimum-Mahalanobis-distance classifier (MMD) and the minimum-Euclidian-distance classifier (MED).
- The maximum-likelihood (ML) classifier and the minimum-Mahalanobis-distance classifier (MMD).
- The maximum-likelihood (ML) classifier and the minimum-Euclidian-distance classifier (MED).

Because there is more than one pair of classification results to be compared for each of the above items, an average Kappa coefficient difference and an average square-root of sum of variances have been calculated for each of them. A Z-value has also been obtained for each item.

The results are shown in Table 3. The higher the Z-value for each item, the more confidence there is that one strategy is significantly different from another. Thus, one can improve the classification accuracy by selecting the best strategy within each step.

As can be seen from Table 3, the largest average Kappa coefficient difference of 0.1124 and the highest Z-value of 3.437 are derived from the results for the two types of training strategy. The second largest average difference of 0.080 with a Z-value of 2.433 is between the ML and the MED. Inclusions of the edge-

TABLE 3. AVERAGE DIFFERENCES OF KAPPA COEFFICIENTS, AVERAGE SQUARE-ROOTS OF THEIR CORRESPONDING SUM OF VARIANCES, AND Z-VALUES

	Average Difference	Square-Root	Z-Value
ST-BT	0.1124	0.0327	3.437
F2-F1	0.0461	0.0327	1.410
F3-F2	0.0370	0.0326	1.135
F4-F3	0.0077	0.0326	0.236
(F4 + F3 − F2 − F1)/2	0.0640	0.0326	1.963
MMD-MED	0.0434	0.0329	1.319
ML-MMD	0.0363	0.0323	1.124
ML-MED	0.0798	0.0328	2.433

Underlining indicates that the difference is significant at the 95 percent confidence level.

density image produce the third largest difference (0.064) with the third highest Z-value. The first three differences all pass the significance test at the 95 percent confidence level.

The fourth largest difference (0.046) results from comparing the two PCA bands with the original XS bands. Although the two PCA bands theoretically should contain 99.6 percent of the variance of the original three XS bands, there is almost a 5 percent accuracy difference between them. The reason for this is not directly apparent to the authors, but two possible explanations are suggested. First, the principal component analysis is based on the assumption that the data set has a unimodal normal distribution. However, this is not the case for the XS data used in this study. Such a violation may alter the elements within the variance-covariance matrix employed to conduct the PCA . The resultant first two PCA images may therefore contain less information than expected. The second explanation is that it may partially result from the quantization made after the PCA transformation. In turn, this could reduce the information content in the PCA image. In other words, the quantized PCA bands contain less feature variance than the expected 99.6 percent of the total feature variance calculated from the original three bands.

SUMMARY AND CONCLUSIONS

In this study, a comparison of the accuracies of different classification procedures for mapping land cover from SPOT HRV data has been presented. Four different combinations of features derived from the SPOT data were used for the analysis. Two types of training strategies were applied to each of the images to generate training statistics for three different classifiers. The results of the classifications were compared by means of three accuracy-assessment procedures.

It is concluded that:

- In all cases, the single-pixel training led to more accurate results than block training at the 95 percent confidence level. Thus, it would appear that single-pixel training is a superior training strategy. However, the analyst requires more time to identify each pixel individually compared with picking out blocks of similar pixels. It should also be noted that the different training strategies can result in very different accuracy estimates for the final classification. Similar results have been reported by Hixson *et al.* (1980) and by Chuvieco and Congalton (1988).
- Different sampling strategies are likely to produce very different accuracy results. In particular, it should be noted that the two random sampling strategies may cause difficulties for the image analyst when the land cover for a mixed pixel is being identified.
- The relatively large classification accuracy difference between the three XS bands and the two PCA bands was not anticipated. It is thought that this might result from the violation of the PCA assumption or the quantization of the PCA bands after the transformation has been performed, but further study is required to determine the reasons.
- The addition of spatial information to the classification statistics by using an edge-density image as an additional image band increases the accuracy of classification. It seems worthwhile to develop simple spatial information extraction methods and test them with higher spatial resolution data such as the SPOT HRV data.

The results of this study indicate that there is a need to establish standardized procedures for measuring and comparing accuracies at all stages of the land classification process. Until a standardized approach becomes available, any accuracy assessment should clearly specify the procedures used.

ACKNOWLEDGMENTS

The authors gratefully acknowledge the assistance of SPOT Image Corporation of France and the Canada Centre for Remote Sensing in supplying the SPOT data used in this study as part of the Programme d'Evaluation Préliminaire SPOT (PEPS), Project No. 229. This research is funded by a Centre of Excellence grant from the Province of Ontario to the Institute for Space and Terrestrial Science and NSERC Operating Grant A0766 awarded to P.J. Howarth. Mr. Gong's studies are supported by the International Development Research Centre (IDRC) of Ottawa. The authors would like to thank Dr. Larry Martin for his helpful discussions on land-cover classification. Also the reviewers' comments are much appreciated.

REFERENCES

Anderson, J. R., E. E. Hardy, J. T. Roach, and R. E. Witmer, 1976. *A Land Use and Land Cover Classification System for Use with Remote Sensor Data*. Professional Paper 964, United States Geological Survey, Washington, D.C.

Campbell J. B., 1981. Spatial correlation effects upon accuracy of supervised classification of land cover. *Photogrammetric Engineering and Remote Sensing*, Vol. 47, No. 3, pp. 355–363.

———, 1987. *Introduction to Remote Sensing*. The Guildford Press, New York, 551 p.

Chuvieco, E., and R. G. Congalton, 1988. Using clustering analysis to improve the selection of training statistics in classifying remotely sensed data. *Photogrammetric Engineering and Remote Sensing*, Vol. 54, No. 9, pp. 1275–1281.

Clark, J., and N. A. Bryant, 1977. Landsat-D Thematic Mapper simulation using aircraft multispectral scanner data. *Proceedings of the 11th International Symposium on Remote Sensing of Environment*, Ann Arbor, Michigan, pp. 483–491.

Cohen, J., 1960. A coefficient of agreement for nominal scales. *Educational and Psychological Measurement*, Vol. 20, No. 1, pp. 37–46.

Fleiss, J. L., J. Cohen, and B. S. Everitt, 1969. Large sample standard errors of Kappa and weighted Kappa, *Psychological Bulletin*, Vol. 72, No. 5, pp. 323–327.

Fung, T., and E. LeDrew, 1988. The determination of optimal threshold levels for change detection using various accuracy indices. *Photogrammetric Engineering and Remote Sensing*, Vol. 54, No. 10, pp. 1449–1454.

Gong, P., and P. J. Howarth, 1989. A modified probabilistic relaxation approach for land-cover classification. *IGARSS'89/12th Canadian Symposium on Remote Sensing*, Vancouver, British Columbia, pp. 1621–1624.

———, 1990. The use of structural information for improving land-cover classification accuracies at the rural-urban fringe. *Photogrammetric Engineering and Remote Sensing*, (in press).

Hixson, M., D. Scholz, N. Fuhs, and T. Akiyama, 1980. Evaluation of several schemes for classification of remotely sensed data. *Photogrammetric Engineering and Remote Sensing*, Vol. 46, No. 12, pp. 1547–1553.

Howarth, P. J., L. R. G. Martin, G. H. Holder, D. D. Johnson, and J. Wang, 1988. SPOT imagery for detecting residential expansion on the rural-urban fringe of Toronto, Canada. *SPOT-1 Image Utilization, Assessment, Results*, Cepadues-Editions, Toulouse, France, pp. 491–498.

Jensen, J. R. (editor), 1983. Urban/Suburban Land Use Analysis. *Manual of Remote Sensing*, Second Edition, R.N. Colwell (editor-in-chief), American Society of Photogrammetry, Falls Church, Virginia, pp. 1571–1666.

Johnson, D. D., and P. J. Howarth, 1987. The effects of spatial resolution on land cover/use theme extraction from airborne digital data. *Canadian Journal of Remote Sensing*, Vol. 13, No. 2, pp. 68–74.

Labovitz, M. L., and E. J. Masuoka, 1984. The influence of autocorrelation in signature extraction—an example from a geobotanical investigation of Cotter Basin, Montana. *International Journal of Remote Sensing*, Vol. 5, No. 2, pp. 315–332.

Latty R. S., R. Nelson, B. Markham, D. Williams, D. Toll, and J. Irons, 1985. Performance comparisons between information extraction techniques using variable spatial resolution data, *Photogrammetric Engineering and Remote Sensing*, Vol. 51, No. 9, pp. 1159–1170.

Lillesand, T. M., and R. W. Kiefer, 1987. *Remote Sensing and Image Interpretation*, Second Edition. John Wiley & Sons, New York, 721 p.

Martin, L. R. G., 1975. *Land Use Dynamics on the Toronto Urban Fringe*.

Lands Directorate Map Folio No. 3, Environment Canada, Ottawa, 47 p.

———, 1986. Change detection in the urban fringe employing Landsat satellite imagery. *Plan Canada*, Vol. 26, No. 7, pp. 182–190.

———, 1989. Accuracy assessment of Landsat-based visual change detection methods applied to the rural-urban fringe. *Photogrammetric Engineering and Remote Sensing*, Vol. 55, No. 2, pp. 209–215.

Martin, L. R. G., P. J. Howarth, and G. Holder, 1988. Multispectral classification of land use at the rural-urban fringe using SPOT data. *Canadian Journal of Remote Sensing*, Vol. 14, No. 2, pp. 72–79.

Richards, J. A., 1986. *Remote Sensing Digital Image Analysis: An Introduction*. Springer-Verlag, Berlin. 281 p.

Rosenfield, G. H., and K. Fitzpatrick-Lins, 1986. A coefficient of agreement as a measure of thematic classification accuracy. *Photogrammetric Engineering and Remote Sensing*, Vol. 52, No. 2, pp. 223–227.

Shimoda, H., and T. Sakata, 1988. Accuracy of landuse classification for SPOT image data. *SPOT-1 Image Utilization, Assessment, Results*, Cepadues-Editions, Toulouse, France, pp. 631–636.

Swain P. H., and S. M. Davis (Eds.), 1978. *Remote Sensing: The Quantitative Approach*. McGraw-Hill, New York. 395 p.

Toll, D. L., 1984. An evaluation of simulated TM data and Landsat MSS data for determining suburban and regional land use and land cover. *Photogrammetric Engineering and Remote Sensing*, Vol. 50, No. 12, pp. 1713–1724.

———, 1985. Effect of Landsat TM sensor parameters on land cover classification. *Remote Sensing of Environment*, Vol. 17, No. 2, pp. 129–140.

Townshend, J., and C. Justice, 1981. Information extraction from remotely sensed data, a user view. *International Journal of Remote Sensing*, Vol. 2, No. 4, pp. 313–329.

Williams, D. L., J. R. Irons, B. L. Markham, R. F. Nelson, and D. L. Toll, 1983. Impact of TM sensor characteristics on classification accuracy. *Proceedings of IGARSS'83*, San Francisco, California, pp. PS1 5.1–5.9.

(Received 14 April 1989; revised and accepted 27 September 1989)